Brilliant Engineering 4 (2020) 26-29

Brilliant Engineering

www.acapublishing.com

RESEARCH ARTICLE

Production, characterization of Fe3O4@CuO composite photocatalysts and determination of photocatalytic activity on Rhodamine B

Hakan Kiziltaş[1] and Derya Tekin[2]

[1] *Department of Chemical Engineering, Ataturk University, Erzurum, Turkey*

[2] *Department of Metallurgy and Materials Engineering, Ataturk University, Erzurum, Turkey*

Abstract

In this study, the hydrothermal method was used to synthesize the Fe_3O_4 particles and the Fe_3O_4@CuO composite photocatalyst. The XRD, SEM-EDS, UV-Vis, and VSM analyzes were used for the characterization of the synthesized particles and composites. The photocatalysts were determined to show typical Fe_3O_4 and CuO properties by XRD analysis which were used to determine the crystal structure of photocatalyst. The SEM analysis was used to investigate the surface morphology of photocatalysts and it was determined that the photocatalysts completed their spherical formation and showed a homogeneous distribution. In addition, the presences of Fe, Cu, and O elements were determined by EDS analysis. The band gap energies of Fe_3O_4 and Fe_3O_4@CuO with UV-Vis measurements were found to be 1.3 and 1.6 eV, respectively. The results of VSM analysis revealed that the Fe_3O_4 and Fe_3O_4@CuO photocatalysts showed approximately the superparamagnetic properties. The degradation of Rhodamine B dye on the photocatalysts was investigated in determining the photocatalytic activities of photocatalysts. The Fe_3O_4@CuO composite photocatalyst showed 76% of dye decomposition.

Keywords: Fe3O4@CuO, photocatalyst, core-shell structure, Rhodamine B, degradation of dye

1. Introduction

Rapidly growing world population and technologies, such as cosmetics, paper, plastic, and textile, cause environmental pollution and especially pollute the water resources rapidly [1]. While the need for water resources has increased due to the increasing world population, the increase in environmental pollution has attracted the attention of the scientific world on water treatment processes [2]. Although physical, chemical, and biological processes are frequently used in water treatment, the search for a new type of decomposition method continues due to the high costs, secondary pollution, and low activities of these processes [3]. Many studies have reported that an alternative method to these traditional methods is heterogeneous photocatalytic processes [4,5].

The developing material technology has been an attractive field of study because of the size and shape-controlled synthesis of metal and metal oxide nanoparticles, which demonstrate different physical and chemical properties [6]. Core-shell structures, which is one of the sizes and shape-controlled synthesis, consist of an inner material (core) and an outer layer material [7]. Core-shell structures have many applications in various technology fields such as photocatalytic degradation of chemical pigments [8], medical imaging [9], biosensors [10], cell labeling [11], solar cells [12], smart drug delivery [13]. The type of material used as core and shell varies depending on the type of application to be used. Therefore, it is possible to intentionally select these materials to obtain the desired performance from the core-shell structures.

Although there are many metal and metal oxide nanoparticles to use the material technology, Copper Oxide (CuO) is often used for various applications such as photocatalyst due to its narrow band gap energy, non-toxic and cheap [14]. CuO is generally synthesis with different methods such as hydrothermal method, microemulsion, and solid vapor phase growth [15].

The biggest disadvantage of using metal and metal oxide particles as photocatalysts is that they are very difficult to recover from the solution medium and cause increased energy losses such as using centrifuged [16]. Failure to recover the entire amount of photocatalyst causes loss of active substance and as a result, greatly increases activity losses.

In recent years, iron (II, III) oxide (Fe_3O_4) has attracted the attention of many researchers as it can be used frequently in many areas because of superior optical, electrical, mechanical, and magnetic properties [17]. Fe_3O_4 is a very important material for the core-shell structure because it is provided to the separation of the composites from the solution medium [18].

In this study, Fe_3O_4@CuO composites were synthesized by the hydrothermal method. The prepared composites were characterized by XRD, SEM-EDS, UV-Vis, and VSM. The photocatalytic properties of the Fe_3O_4@CuO composites were investigated on the Rhodamine B dye solution.

2. Experimental

2.1. Materials

The chemicals for used production of Fe3O4 particles were FeCI3.6H2O (iron (III) chloride hexahydrate, Sigma Aldrich, 98%), C2H6O2 (ethylene glycol, Sigma Aldrich, 98%), C2H3NaO2 (sodium acetate, Sigma Aldrich,

*Corresponding Author: deryatekin@atauni.edu.tr
(D. Tekin Orcid: 0000-0002-2094-3474)

Received 5 May 2020 Revised 12 May 2020 Accepted 18 May 2020
Brilliant Enginering 4 (2020) 26-29
https://doi.org/10.36937/ben.2020.004.005

99%), C2nH4n+2On+1 (polyethylene glycol, Sigma Aldrich, Mr 7000-9000), and distilled water.

The chemicals for used production of Fe3O4@CuO composites were CuSO4.5H2O (Copper (II) sulfate pentahydrate, Sigma Aldrich, 98%), C2H5OH (Ethanol, Sigma Aldrich, 99.8%), NaOH (Sodium hydroxide, Sigma Aldrich, 98%), and distilled water.

2.2. Synthesis of Fe_3O_4 particles

The hydrothermal method was used for Fe_3O_4 synthesis [19]. 5.6 g iron (III) chloride hexahydrate in 80 ml ethylene glycol (EG) were ultrasonically dissolved and 14.4 g sodium acetate and 4 g polyethylene glycol (PEG) were added to the solution. The stirring was continued ultrasonically until a homogeneous solution was obtained, and the solution was transferred to the Teflon autoclave reactor and kept in the oven for 12 hours at 200°C. At the end of the treatment, the prepared Fe_3O_4 particles were separated from the solution in the Teflon reactor cooled to room temperature by an external magnet. The obtained particles were washed three times with distilled water and ethanol and dried in an oven at 60°C for 3 hours.

2.3. Synthesis of Fe_3O_4@CuO composites

The hydrothermal method was used for Fe_3O_4@CuO synthesis [20]. 2 g of Fe_3O_4 particles was ultrasonically dissolved in a solution containing 20 ml of water and 100 ml of ethanol. Then, 8.9 g of $CuSO_4.5H_2O$ and 3.5 g of NaOH were added to the solution medium, and the stirring continued until a homogeneous solution was obtained. Then, the solution was transferred to the Teflon autoclave reactor and kept in the oven for 12 hours at 200°C. At the end of the heat treatment, the prepared Fe_3O_4@CuO composites were separated from the solution in the Teflon reactor cooled to room temperature by an external magnet. The obtained composites were washed three times with distilled water and ethanol and dried in an oven at 60°C for 3 hours.

2.4. Characterization

Scanning Electron Microscope (SEM, Zeiss -Sigma 300), Energy Dispersive X-ray Spectroscopy (EDS), X-ray diffraction (XRD, PANalytical-Empyrean), UV-Visible Spectrophotometer (UV, Shimadzu-UV3600 Plus), and Vibrating Sample Magnetometer (VSM, Lake Shore, 7407) analyzes were used for the characterization of the produced Fe_3O_4 particles and Fe_3O_4@CuO composites.

2.5. Photocatalytic performance

The photocatalytic activity experiments of the produced composite photocatalysts were carried out in a light-insulated batch reactor. The saturated O_2 concentration of the solution medium was provided by an air pump. A water circulator was used to keep the reaction medium temperature constant at 25°C. The UV lamp (257 nm, 44 W/m^2) was used as a light source. In all experiments, 100 mg of photocatalyst and 20 ppm and 400 ml of Rhodamine B dye solution were used. Before the photocatalytic experiment, the photocatalyst was added to the dye solution and kept in the dark environment for 30 minutes to ensure the adsorption-desorption equilibrium. The solution concentration at the determined different times was determined using the UV spectrophotometer (Optizenα spectrophotometer) during the experiment.

3. Result and Discussion

The XRD patterns of the synthesized Fe_3O_4 particles and Fe_3O_4@CuO composites were shown in Figure 1.

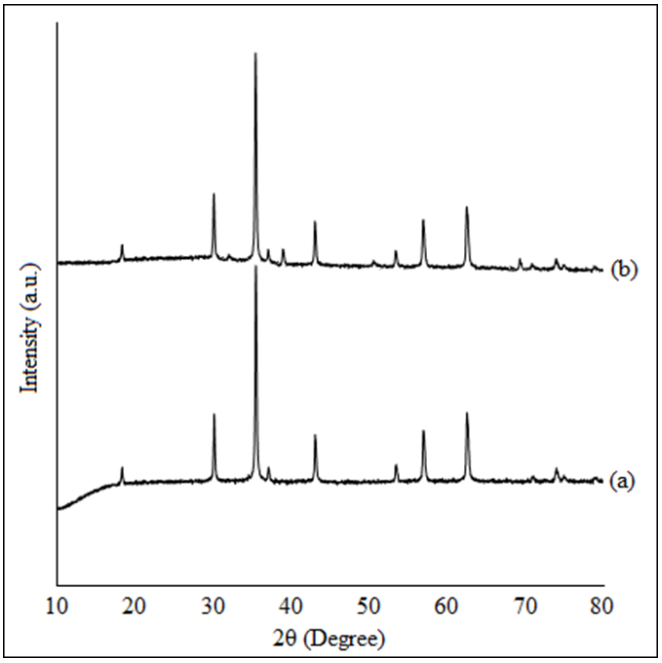

Figure 1. XRD results of (a) Fe_3O_4 particles and (b) Fe_3O_4@CuO composites

The XRD pattern of Fe_3O_4 was shown in Figure 1a. The diffraction peak at 2θ = 18.50, 30.38, 35.70, 43.36, 53.84, 57.36, 63.00, and 74,48° were about Fe_3O_4 sample are related to (111), (220), (311), (400), (422), (511), (440), and (533) planes, which are about the cubic spinel-structured magnetite (JCPDS:19-0629) [21]. When Figure 1b shows the XRD result of the Fe3O4@CuO composites was examined, besides Fe3O4 peaks, the new diffraction peaks at 2θ =31.8, 39.3, 51.5, and 68.2°, which were indexed with the monoclinic phase of CuO, are associated to (110), (111), (020), and (311) planes [22]. The calculated average particle size of the Fe_3O_4 particles and Fe_3O_4@CuO composites by using the formula of Debye-Scherrer [23] was 207 and 309 nm, respectively.

The SEM and EDS results of the synthesized Fe_3O_4 particles and Fe_3O_4@CuO composites were shown in Figure 2.

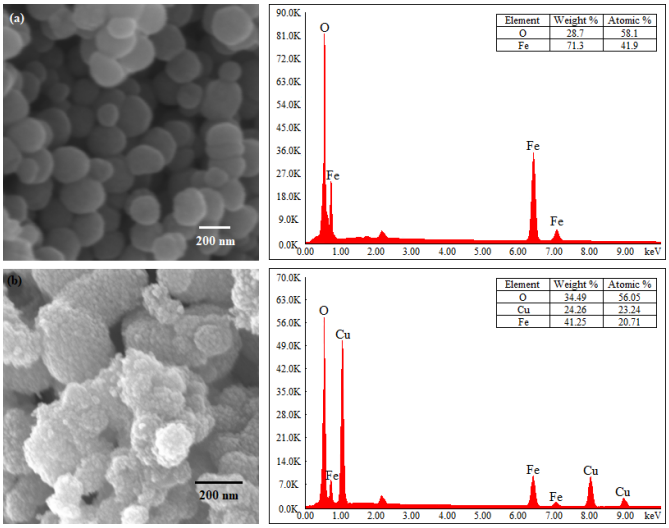

Figure 2. SEM results of (a) Fe_3O_4 particles and (b) Fe_3O_4@CuO composites

The results of the SEM analysis of Fe_3O_4 particles were shown in Figure 2a. When the results of the SEM analysis of Fe_3O_4 particles were examined in Figure 2a, Fe_3O_4 particles have completed their spherical formation and show a homogeneous distribution. The average diameter of the Fe_3O_4 particles is 210 nm and the diameter

distributions are in the range of 150 to 250 nm. It proved the presence of Fe and O in the sample of Fe_3O_4 with the EDS analysis. As shown in Figure 2b, the Fe_3O_4@CuO composites have completed their formation, but they do not show uniform structure since the agglomeration occurs. The average diameter of the Fe_3O_4@CuO composites is 260 nm and the diameter distributions are in the range of 160 to 320 nm. It proved the presence of Fe, O, and Cu in the sample of Fe_3O_4@CuO with the EDS analysis.

The vibrating sample magnetometry measurements were used to determine the magnetic properties of Fe_3O_4 particles and Fe_3O_4@CuO composites and the results were shown in Figure 3.

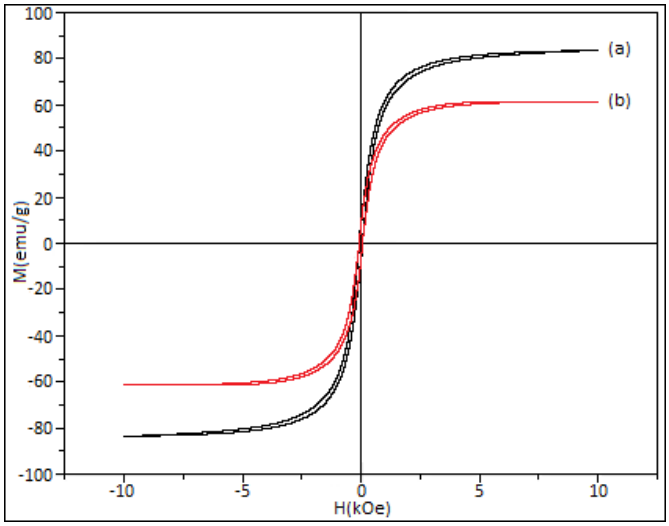

Figure 3. VSM analyze results of (a) Fe_3O_4 particles and (b) Fe_3O_4@CuO composites

The saturation values of magnetization (M) of the Fe_3O_4 particles and Fe_3O_4@CuO core-shell composites were measured to be 81 and 62 emu.g^{-1}, respectively, and exhibited nearly the properties of superparamagnetic [24]. The coating of CuO caused a decrease in the magnetization value of Fe_3O_4, this decrease in magnetization value of Fe_3O_4 can be shown as evidence that CuO was coated on the surface of Fe_3O_4.

The absorbance measurements of Fe_3O_4 particles and Fe_3O_4@CuO composite were determined by the UV spectrophotometer and the band gap energies were calculated by using the Tauc method [25], as shown in Figure 4.

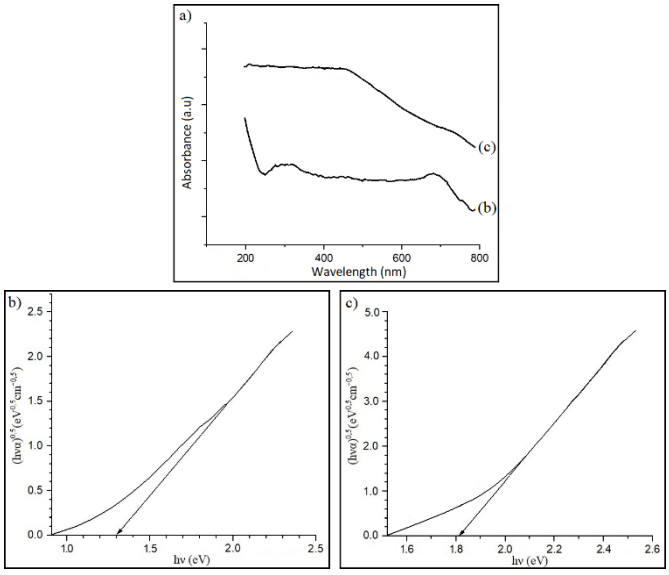

Figure 4. (a) The spectrum of UV–Vis absorption of the Fe_3O_4 and Fe_3O_4@CuO, the results of Tauc plot of **(b)** Fe_3O_4 **(c)** Fe_3O_4@CuO

Figure 4a shows the UV-Vis absorption spectrum for the Fe_3O_4 and Fe_3O_4@CuO. The band gap energies of Fe_3O_4 particles and Fe_3O_4@CuO composite were determined with the intercept of the tangents to the plots of $(h\upsilon\alpha)^{0.5}$ vs $(h\upsilon)$, as shown in Figure 4a -b. The estimated band gap energies (E_g) of Fe_3O_4 particles and Fe_3O_4@CuO composite is 1.3 and 1.81 eV.

The photocatalytic activity experiments of Fe_3O_4 particles and Fe_3O_4@CuO composites were investigated on the degradation of Rhodamine B dye and shown in Figure 5.

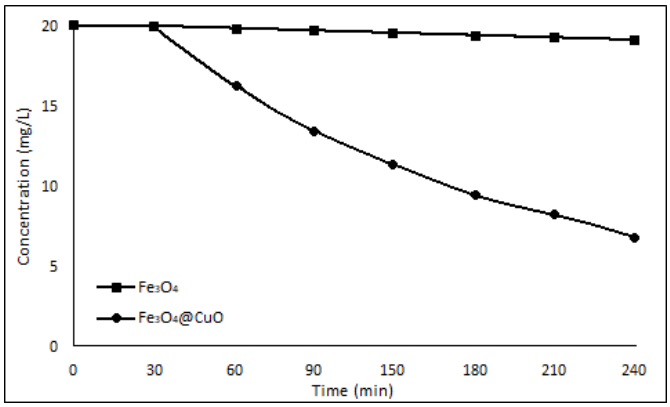

Figure 5. The results of photocatalytic activity experiments

After the dye solution and photocatalysts were added to the reaction medium, the solution was kept in the dark environment for the first 30 minutes to establish an adsorption equilibrium. The solution concentration did not change significantly in dark environment experiments. In experiments carried out under UV light, the Fe_3O_4 particles were able to decompose 13% of Rhodamine B, while the dye decomposition of the Fe_3O_4@CuO composite was about 76%.

4. Conclusion

The Fe_3O_4 particles and the Fe_3O_4@CuO composite photocatalyst were synthesized by using the hydrothermal method. The characterization of the synthesized particles and composites was carried out by using XRD, SEM-EDS, UV-Vis, and VSM analyzes. The crystal structure of produced photocatalysts were determined by XRD analysis, the samples were showed the typical Fe_3O_4 and CuO properties. It was determined by SEM analysis that photocatalysts completed their global formation and demonstrated homogeneous distribution, and the average particle sizes were 207 and 309 nm for Fe_3O_4 and Fe_3O_4@CuO, respectively. Besides, the EDS analysis was proven the presences of Fe, Cu, and O elements. The optic band gap energies of Fe_3O_4 and Fe_3O_4@CuO with UV-Vis measurements were found to be 1.3 and 1.6 eV, respectively. The results of VSM analysis revealed that the Fe_3O_4 and Fe_3O_4@CuO photocatalysts showed approximately the superparamagnetic properties. The degradation of Rhodamine B dye on the photocatalysts was investigated in determining the photocatalytic activities of photocatalysts. The Fe_3O_4@CuO composite photocatalyst showed 76% of dye decomposition.

Declaration of Conflict of Interests

The authors declare that there is no conflict of interest.

References

[1.] Kiziltaş, H., Tekin, T., Increasing of Photocatalytic Performance of TiO_2 Nanotubes by Doping AgS and CdS. Chemical Engineering Communications 204 (2017) 852-857.

[2.] Jury, W.A., Vaux, H., The role of science in solving the world's emerging water problems. Proceedings of the National Academy of Sciences of the United States of America 102 (2005) 15715-15720.

[3.] Rasalingam, S., Peng, R., Koodali, R.T., Removal of Hazardous Pollutants from Wastewaters: Applications of TiO_2-SiO_2/ Mixed Oxide Materials. Journal of Nanomaterials 2014 (2014) 617405.

[4.] Chen, D., Muthusamy, S., Ray, A., Heterogeneous Photocatalysis in Environmental Remediation. Developments in Chemical Engineering and Mineral Processing 8 (2008).

[5.] Ibhadon, A.O., Fitzpatrick, P., Heterogeneous photocatalysis: recent advances and applications. Catalysts 3 (2013) 189-218.

[6.] Khan, I., Saeed, K., Khan, I., Nanoparticles: Properties, applications and toxicities. Arabian Journal of Chemistry 12 (2019) 908-931.

[7.] Gawande, D.M., Goswami, A., Asefa, T., Guo, H., Biradar, A., Peng, D.-L., Zboril, R., Varma, R., Core–shell nanoparticles: synthesis and applications in catalysis and electrocatalysis. Chemical Society Reviews 44 (2015) 7540-7590.

[8.] Kiziltaş, H., Tekin, T., Tekin, D., Preparation and characterization of recyclable Fe_3O_4@SiO_2@TiO_2 composite photocatalyst, and investigation of the photocatalytic activity. Chemical Engineering Communications (2020) 1-13.

[9.] Lai, C.W., Wang, Y.H., Lai, C.H., Yang, M.J., Chen, C.Y., Chou, P.T., Chan, C.S., Chi, Y., Chen, Y.C., Hsiao, J.K., Iridium-complex-functionalized Fe_3O_4/SiO_2 core/shell nanoparticles: a facile three-in-one system in magnetic resonance imaging, luminescence imaging, and photodynamic therapy. Small 4 (2008) 218-224.

[10.] Zhang, Y., Zeng, G.-M., Tang, L., Huang, D.-L., Jiang, X.-Y., Chen, Y.-N., A hydroquinone biosensor using modified core–shell magnetic nanoparticles supported on carbon paste electrode. Biosensors and Bioelectronics 22 (2007) 2121-2126.

[11.] Shinde, S., El-Schich, Z., Malakpour, A., Wan, W., Dizeyi, N., Mohammadi, R., Rurack, K., Gjörloff Wingren, A., Sellergren, B.r., Sialic acid-imprinted fluorescent core–shell particles for selective labeling of cell surface glycans. Journal of the American Chemical Society 137 (2015) 13908-13912.

[12.] Li, Z., Liang, X., Li, G., Liu, H., Zhang, H., Guo, J., Chen, J., Shen, K., San, X., Yu, W., 9.2%-efficient core-shell structured antimony selenide nanorod array solar cells. Nature communications 10 (2019) 1-9.

[13.] Lin, C., Sun, K., Zhang, C., Tan, T., Xu, M., Liu, Y., Xu, C., Wang, Y., Li, L., Whittaker, A., Carbon dots embedded metal organic framework@ chitosan core-shell nanoparticles for vitro dual mode imaging and pH-responsive drug delivery. Microporous and Mesoporous Materials 293 (2020) 109775.

[14.] Zoolfakar, A., Abdul Rani, R., Morfa, A., O'Mullane, A., Kalantar-zadeh, K., Nanostructured copper oxide semiconductors: A perspective on materials, synthesis methods and applications. J. Mater. Chem. C 2 (2014).

[15.] Davarpanah, S.J., Karimian, R., Piri, F., Synthesis of copper (II) oxide (CuO) nanoparticles and its application as gas sensor. Journal of Applied Biotechnology Reports 2 (2015) 329-332.

[16.] Moma, J., Baloyi, J., Modified Titanium Dioxide for Photocatalytic Applications, in: Photocatalysts-Applications and Attributes. IntechOpen, 2018.

[17.] Shi, D., Dunn, A., Mast, D., Photo-fluorescent and magnetic properties of iron oxide nanoparticles for biomedical applications. Nanoscale 7 (2015) 8209-8232.

[18.] Liang, L., Zhu, Q., Wang, T., Wang, F., Ma, J., Jing, L., Sun, J., The synthesis of core–shell Fe_3O_4@mesoporous carbon in acidic medium and its efficient removal of dye. Microporous and Mesoporous Materials 197 (2014) 221–228.

[19.] Ahmadi, S., Chia, C.-h., Zakaria, S., Saeedfar, K., Asim, N., Synthesis of Fe_3O_4 nanocrystals using hydrothermal approach. Journal of Magnetism and Magnetic Materials 324 (2012) 4147–4150.

[20.] Zhang, Y.-F., Qiu, L.-G., Yuan, Y.-P., Zhu, Y.-J., Jiang, X., Xiao, J.-D., Magnetic Fe_3O_4@C/Cu and Fe_3O_4@CuO core–shell composites constructed from MOF-based materials and their photocatalytic properties under visible light. Applied Catalysis B: Environmental 144 (2014) 863-869.

[21.] Ao, L., Hu, X., Xu, M., Zhang, Q., Huang, L., Central-radial bi-porous nanocatalysts with accessible high unit loading and robust magnetic recyclability for 4-nitrophenol reduction. Dalton Transactions 49 (2020) 4669-4674.

[22.] Aryanasab, F., A magnetically recyclable iron oxide-supported copper oxide nanocatalyst (Fe_3O_4–CuO) for one-pot synthesis of S-aryl dithiocarbamates under solvent-free conditions. RSC advances 6 (2016) 32018-32024.

[23.] Straasø, T., Becker, J., Iversen, B.B., Als-Nielsen, J., The Debye–Scherrer camera at synchrotron sources: a revisit. Journal of synchrotron radiation 20 (2013) 98-104.

[24.] Jung, C.W., Jacobs, P., Physical and chemical properties of superparamagnetic iron oxide MR contrast agents: ferumoxides, ferumoxtran, ferumoxsil. Magnetic resonance imaging 13 (1995) 661-674.

[25.] Viezbicke, B.D., Patel, S., Davis, B.E., Birnie III, D.P., Evaluation of the Tauc method for optical absorption edge determination: ZnO thin films as a model system. physica status solidi (b), 252 (2015) 1700-1710.

How to Cite This Article

Kiziltas, H., and Tekin, D., Production, characterization of Fe_3O_4@CuO composite photocatalysts and determination of photocatalytic activity on Rhodamine B, Brilliant Engineering, 4(2020), 26-30.